Supplementary Material

Inventory of supplemental items:

Supplemental Figures and Figure legend:

Figure S1, related to Figures 2, 3 and Experimental procedures: Characterization of Tpr assembly and dynamics in WT and *Nup133*$^{-/-}$ mESC lines

Figure S2, related to Figure 4: GFP-Nup153 levels and dynamics in WT versus *Nup133*$^{-/-}$ mESCs

Figure S3, related to Figure 5: Expression and localization of the GFP-Nup133 fusions used in Fig 5B and Tpr localization at the NE in refined Nup133ΔMid mutants.

Supplemental Tables:

Table S1, related to Experimental Procedures**.** Plasmids used in this study

Table S2, related to Experimental Procedures. Cell lines used in this study

Table S3, related to Experimental Procedures. Sequences of gRNAs and Primers used in this study

Table S4, related to Experimental Procedures. Antibodies used in this study, related to Experimental Procedures

Supplemental Experimental Procedures:

Plasmids

mESC lines derivation, growth conditions, and transfection

Real-time quantitative PCR

Detailed procedures from High Resolution Imaging (3D SIM): immunostaining, image acquisition and processing

Western blot analyses

Pull-down experiments and mass spectrometry analyses

References to Supplemental Tables and Experimental Procedures

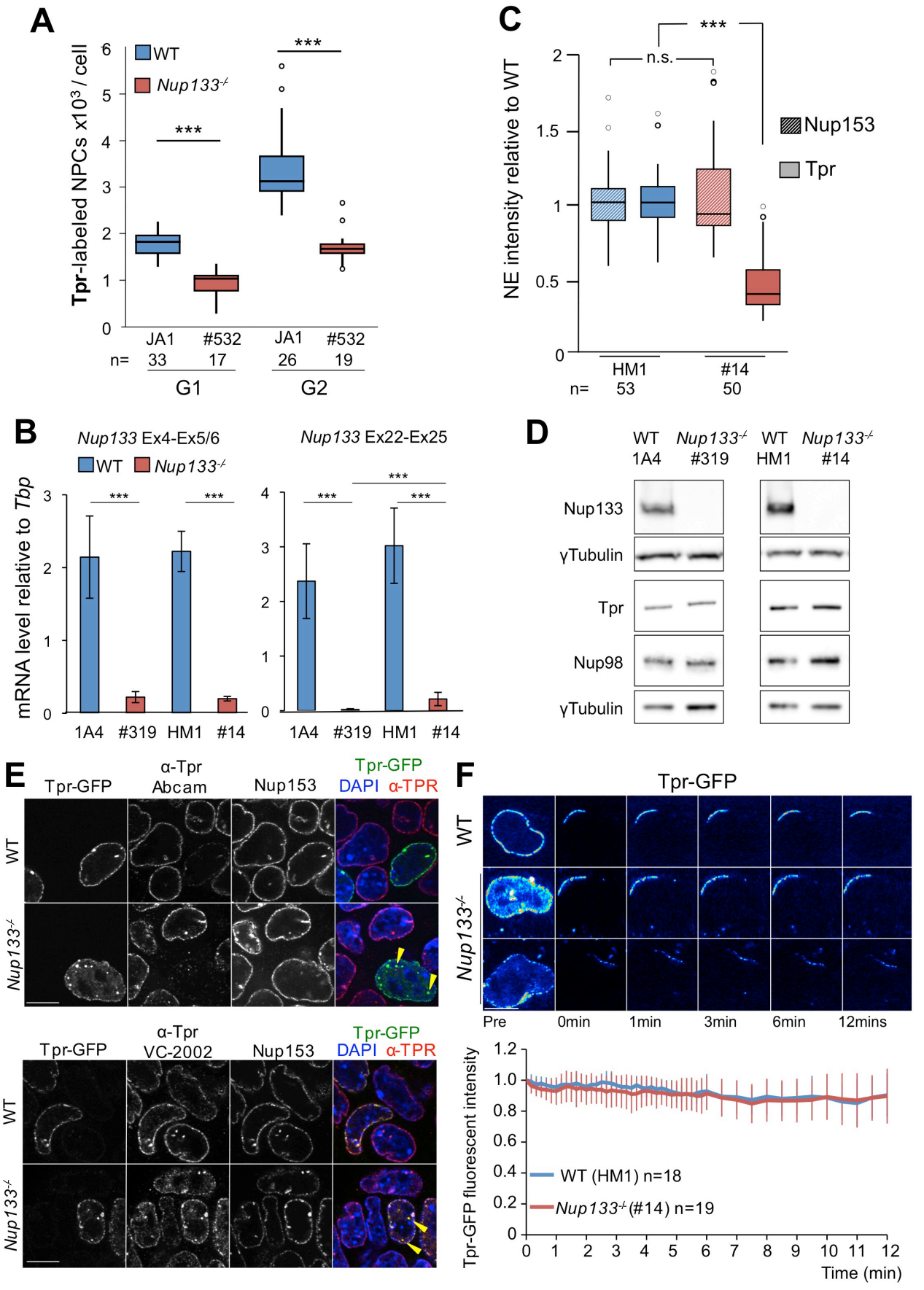

Figure S1, related to Figures 2, 3 and Experimental Procedures (see legend on next page)

Figure S1, related to Figures 2 and 3: Characterization of Tpr assembly and dynamics in WT and *Nup133*$^{-/-}$ mESC lines.

A. 3D SIM- and Imaris-based quantification of the total number of Tpr-labeled NPCs in WT (JA1) and *Nup133*$^{-/-}$ (#532) mESCs during G1 and G2. **B.** *Nup133* mRNA level relative to Tbp expression was determined by RT-QPCR on pluripotent WT and *Nup133*$^{-/-}$ mESCs. Two primer pairs, in exon 4 (forward)-exons 5/6 (reverse) and in exon 22 (forward)-exon 25 (reverse), were used. At least 4 independent samples of each cell line per primer pair were analyzed. The *Nup133*^{merm} allele in #319 and the *Nup133*$^{\Delta 2\text{-}6}$ & *Nup133*$^{\Delta 6}$ alleles in #14 (see Experimental procedures) encode premature stop codons, resulting in non-sense mediated mRNA decay. The Nup133 Ex22-Ex25 primer pair does not detect the *Nup133*^{merm} allele since this allele caries a point mutation at the first base of intron 22 that leads to exon 22 skipping. The Nup133 ex4-ex5-6 primer pair is not present in the *Nup133*$^{\Delta 2\text{-}6}$ allele but recognizes the *Nup133*$^{\Delta 6}$ allele in #14. **C.** Normalized Nup153 and Tpr signal intensities at the NE of WT (HM1) and *Nup133*$^{-/-}$ (#14) mESCs. Data obtained from spinning disk confocal images of cells co-labeled with Nup153, Tpr and Nup133 antibodies as in Fig 3A. n: number of cells quantified from ≥ two independent experiments. **D.** Western analysis of Nup133, Tpr and Nup98 protein level in WT and *Nup133*$^{-/-}$ mESCs. Gamma-Tubulin was used as loading control. **E.** Representative images of WT (HM1) and *Nup133*$^{-/-}$ (#14) mESCs transiently expressing Tpr-GFP and stained with anti-Nup153 and two distinct anti-Tpr antibodies. The overlays reveal intranuclear foci stained by Tpr-GFP and the Tpr antibodies but not by Nup153 antibody (arrowheads). Bar 10μm. Top; The Abcam antibody directed against the C-terminal amino acids of Tpr (2300-2349) does not recognize Tpr-GFP, which contains GFP fused to the C-terminus of Tpr. Thus, the decreased Abcam anti-Tpr signal observed in Tpr-GFP expressing cells indicates that the Tpr-GFP fusion replaced endogenous Tpr within the NPCs. Bottom; fluorescence analyses using the VC-2002 anti-Tpr antibody, which recognizes both endogenous Tpr and the transiently transfected Tpr-GFP, indicate that transient expression of the GFP fusion does not noticeably increase the total level of Tpr at the NE. **F.** Top; selected pseudocolored images (each an average projection of 3 z-sections) from different time points during iFRAP experiments performed on WT (HM1) and *Nup133*$^{-/-}$ (#14) mESCs transfected with Tpr-GFP. Two distinct *Nup133*$^{-/-}$ mESCs with different Tpr-GFP intensities are shown. Scale bar, 10μm. Bottom; plots of fluorescence decay from the unbleached NE regions in these iFRAP experiments. Each curve represents the mean ± S.D, of n cells acquired in 2 independent experiments.

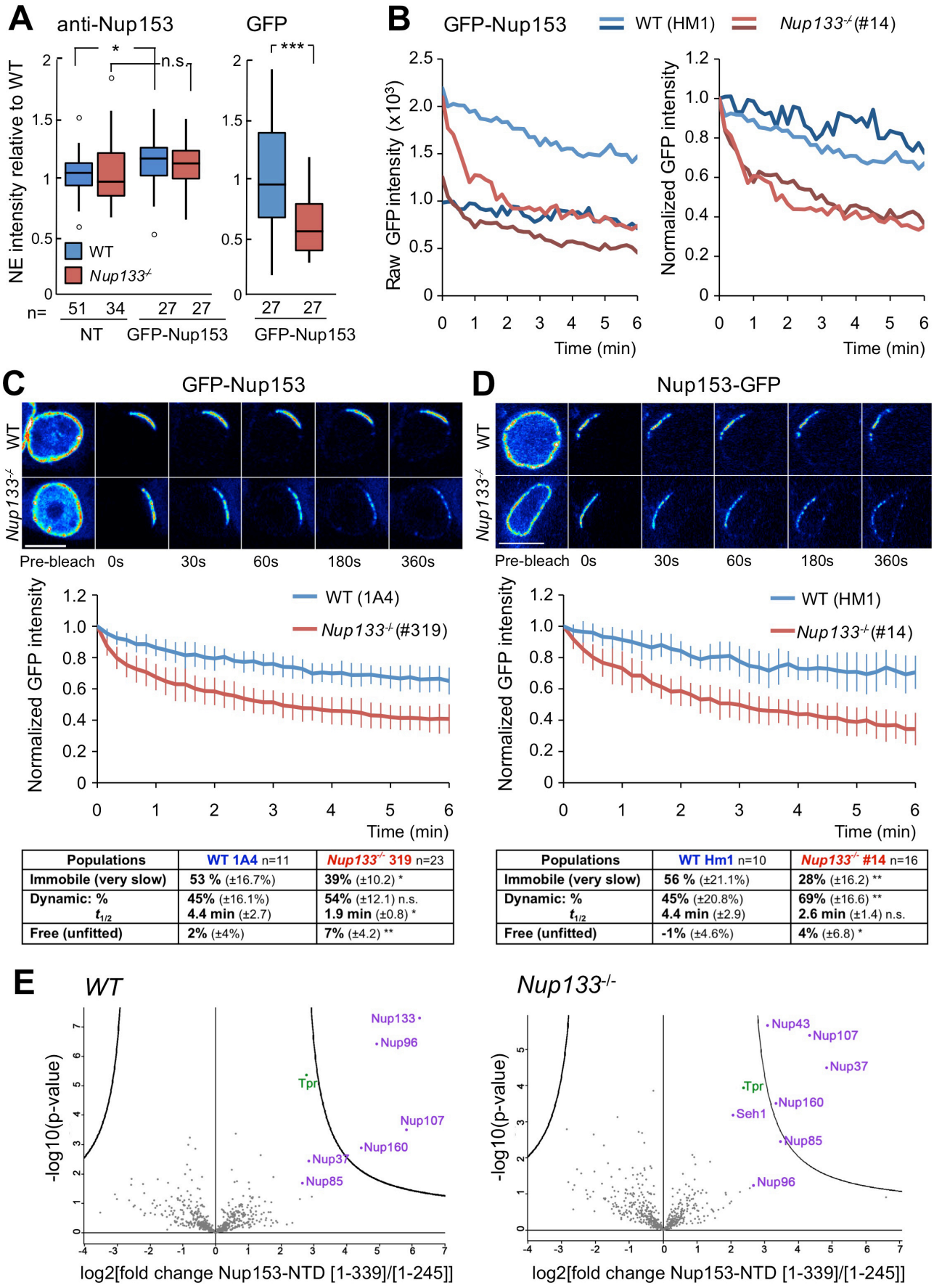

Populations	WT 1A4 n=11	Nup133-/- 319 n=23
Immobile (very slow)	53 % (±16.7%)	39% (±10.2) *
Dynamic: %	45% (±16.1%)	54% (±12.1) n.s.
$t_{1/2}$	4.4 min (±2.7)	1.9 min (±0.8) *
Free (unfitted)	2% (±4%)	7% (±4.2) **

Populations	WT Hm1 n=10	Nup133-/- #14 n=16
Immobile (very slow)	56 % (±21.1%)	28% (±16.2) **
Dynamic: %	45% (±20.8%)	69% (±16.6) **
$t_{1/2}$	4.4 min (±2.9)	2.6 min (±1.4) n.s.
Free (unfitted)	-1% (±4.6%)	4% (±6.8) *

Figure S2, related to Figure 4 (see legend on next page)

Figure S2, related to Figure 4. GFP-Nup153 levels and dynamics in WT versus *Nup133*$^{-/-}$ mESCs

A. Total NE levels of Nup153 are not significantly increased upon transient expression of GFP-Nup153 in mESCs. WT (HM1) and *Nup133*$^{-/-}$ (#14) mESCs, either non-transfected (NT) or transiently expressing GFP-Nup153, were immunolabeled using anti-Nup153 antibody. Signal intensities at the NE were quantified for total Nup153 (endogenous + GFP-Nup153) (left) and for GFP (right) and values were normalized in each field relative to non-transfected WT mESCs and to GFP-Nup153 transfected WT mESCs, respectively. Average ± S.D., of n cells acquired in 2 independent experiments. **B.** Plots of fluorescence decay kinetics of GFP-Nup153 from the unbleached NE region in two distinct WT (HM1, blue curves) and two distinct *Nup133*$^{-/-}$ (#14, red curves) mESCs before (left) and after (right) normalization to 1 at the first time point after bleach (defined at t=0). Note that despite the variable GFP intensities inherent to transient transfections, the curves become very comparable for a given genotype following normalization. This indicates that the initial amount of GFP-Nup153 at the NE does not affect the decay profiles. **C-D.** Top; pseudocolored images of selected time frames from representative iFRAP experiments performed on WT (1A4) or *Nup133*$^{-/-}$ (#319) mESCs expressing GFP-Nup153 (**B**), and on WT (HM1) or *Nup133*$^{-/-}$ (#14) mESCs expressing Nup153-GFP (**C**). Time 0 was defined as the first time point after bleach. Scale bar, 10μm. Middle; plots of fluorescence decay kinetics from the unbleached region in WT (blue curves) and *Nup133*$^{-/-}$ (red curves) mESCs. Average normalized fluorescence signals ± SDs were quantified at each acquisition time point as detailed in Experimental Procedures. Bottom; the number of cells (n=, acquired in 2 independent experiments) used for the graphs and curve fitting is indicated. Fractions of the various GFP-Nup153 and Nup153-GFP populations exhibiting distinct dynamics at the NE and the half time of residency for the dynamic population ($t_{1/2}$) were determined based on the fit of the normalized fluorescence signals from the indicated number of WT or *Nup133*$^{-/-}$ (see Experimental Procedures) **E.** Volcano plots of the quantitative mass spectrometry analysis of pull-down experiments revealing magnitude and significance of the cellular proteins interacting with Nup153-NTD [aa 1-339] compared to [aa 1-245] in (left) WT (HM1) and (right) *Nup133*$^{-/-}$ (#14) mESCs. The curves correspond to the 5% threshold cut-offs. Points corresponding to Y-complex Nups and Trp are highlighted.

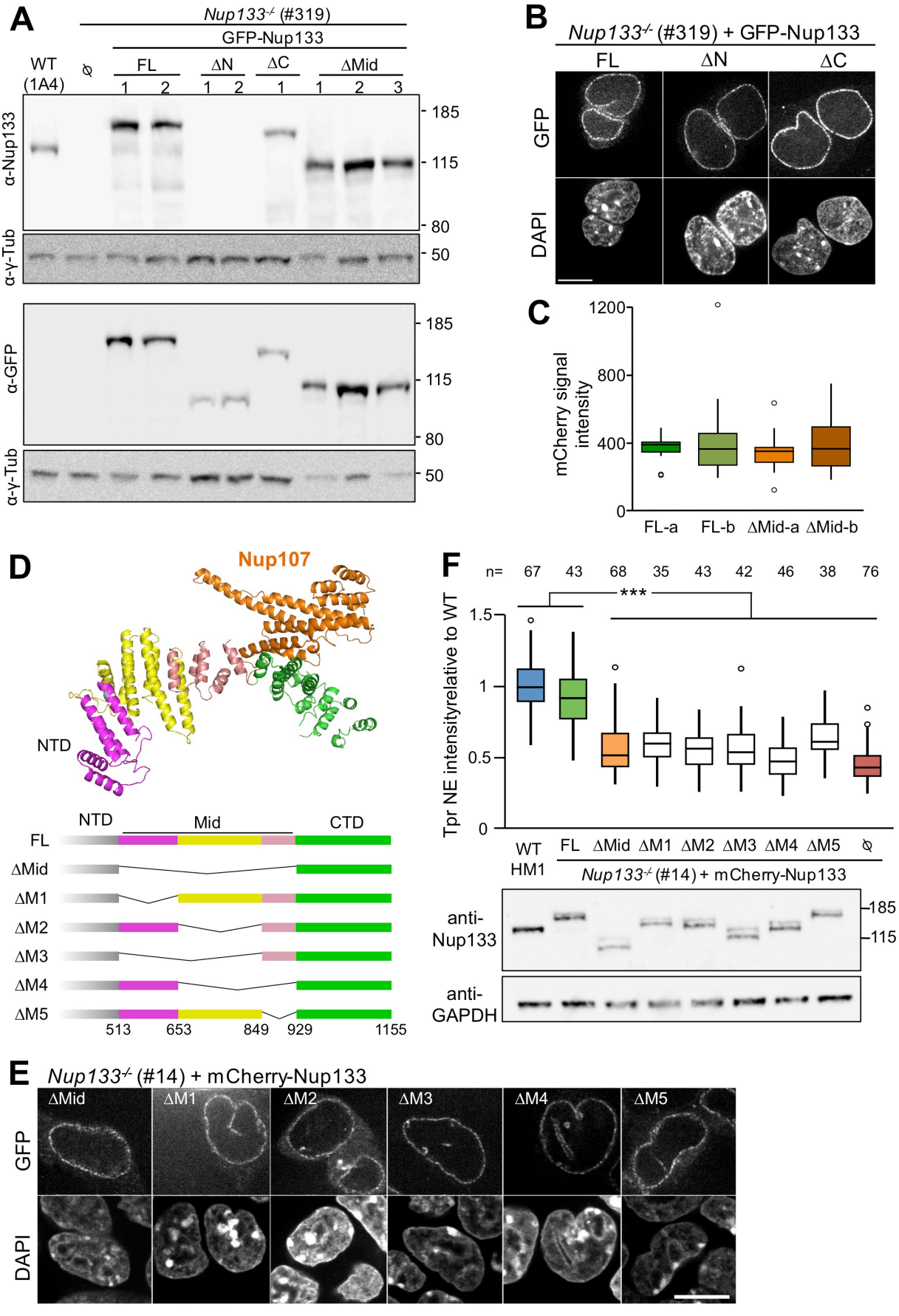

Figure S3, related to Figure 5 (see legend on next page)

Figure S3, related to Figure 5: Expression and localization of the GFP-Nup133 fusions used in Fig 5B and Tpr localization at the NE in refined Nup133ΔMid mutants.

A. Whole cell extracts from the various mESC clones from Fig 5B were analyzed by western blot using an anti-NTD-Nup133 (top) and an anti-GFP (bottom) antibodies. Anti-gamma-Tubulin is used as loading control. Note that as anticipated, the GFP-Nup133ΔN fusion is solely recognized by the anti-GFP antibody. **B.** Fluorescence analysis of representative *Nup133*$^{-/-}$ (#319) mESC clones stably expressing GFP-Nup133 FL, ΔN and ΔC (from Fig 5B). The GFP signal and DAPI are shown. Bar, 10μm. **C.** mCherry fluorescent levels at the NE of *Nup133*$^{-/-}$ mESCs (#14) stably expressing mCherry-Nup133-FL or ΔMid (from Fig 5E). **D**. The structure of Nup133-Mid-CTD and its direct partner, Nup107-CTD (adapted from Whittle and Schwartz, 2009) color-coded to depict the helices deleted in the five Nup133ΔMid constructs (ΔM1 to ΔM5) schematized below and used in (E-F)**. E**. Fluorescence analysis of representative *Nup133*$^{-/-}$ (#14) mESCs transiently expressing the various GFP-Nup133ΔMid constructs. The GFP signal and DAPI are shown. Bar, 10μm. **F**. Top; normalized Tpr signal intensity at the NE in WT (HM1) and *Nup133*$^{-/-}$ (#14) mESCs, either control (Ø) or transiently expressing the indicated mCherry-Nup133 FL or ΔMid constructs. The numbers of cells quantified (n) indicated come from two distinct experiments. Bottom; whole cell extracts from mESCs transiently expressing the mCherry-Nup133 FL or the indicated ΔMid constructs were analyzed by western blot using anti-Nup133-NTD and anti-GAPDH antibodies.

Supplemental Tables

Table S1, related to Experimental Procedures. **Plasmids used in this study** (sequences are available upon request).	SOURCE	IDENTIFIER
pCAG-GFP-mNup133-IRES-puro	This paper	#1642
pCAG-GFP-mNup133ΔN-IRES-puro (ΔN, Δ aa 1-501)	This paper	#1656
pCAG-GFP-mNup133ΔMid-IRES-puro (ΔMid, Δaa 513-929)	This paper	#1919
pCAG-GFP-mNup133ΔC-IRES-puro (ΔC, Δaa 1024-1155)	This paper	#1657
pCAG-mCherry-mNup133-IRES-puro	This paper	#1937
pCAG-mCherry-mNup133ΔMid-IRES-puro (ΔMid, Δ aa 513-929)	This paper	#1938
pCAG-mCherry-mNup133ΔMid1-IRES-puro (ΔM1, Δ aa 513-653)	This paper	#1974
pCAG-mCherry-Nup133ΔMid2-IRES-puro (ΔM2, Δ aa 653-849)	This paper	#1975
pCAG-mCherry-Nup133ΔMid3-IRES-puro (ΔM3, Δ aa 513-849)	This paper	#1976
pCAG-mCherry-Nup133ΔMid4-IRES-puro (ΔM4, Δ aa 653-929)	This paper	#1977
pCAG-mCherry-Nup133ΔMid5-IRES-puro (ΔM5, Δ aa 849-929)	This paper	#1978
pCMV-GFP_{3x}-Nup153	(Rabut et al., 2004)	Euroscarf #P30458
pCMV-Nup153-GFP_{3x}	This paper	#1991
pCMV-GFP_{3x}-Nup153-NTD [aa 1-339]	This paper	#1959
pCAG-Tpr-GFP	This paper	#2040
pET28a-zz-hNup153 [aa 1-245]	From D. Forbes (Vasu et al., 2001)	N/A
pET28a-zz-hNup153 [aa 1-339]	From D. Forbes (Vasu et al., 2001)	N/A
pX-98: U6p-gRNA(mNup133#1)_U6p-gRNA(mNup133#2)_CMVp-nCas9-EGFP_SV40p-PuroR-pA)(gRNAs within mNup133 exon 6)	This paper	pX-98
pX-102: U6p-tru gRNA(mNup133#5)_U6p-tru gRNA(mNup133#6)_CMVp-Cas9-mCherry_SV40p-PuroR-pA) (tru gRNAs flanking Nup133 exon 2)	This paper	pX-102

Table S2, related to Experimental Procedures. **Cell Lines used in this study:**	SOURCE	IDENTIFIER
Mouse embryonic fibrobast DR4	Applied StemCell	ASF-1001
Mouse embryonic stem cell 1A4 WT *Sox1*$^{gfp/+}$	This paper	N/A
Mouse embryonic stem cell JA1 WT *Sox1*$^{gfp/+}$	This paper	N/A
Mouse embryonic stem cell #319 *Nup133*$^{merm/merm}$; *Sox1*$^{gfp/+}$	This paper	N/A
Mouse embryonic stem cell #532 *Nup133*$^{merm/merm}$; *Sox1*$^{gfp/+}$	This paper	N/A
Mouse embryonic stem cell HM1 (WT)	ThermoFisher Scientific (Selfridge et al., 1992)	MES4303
Mouse embryonic stem cell HM1 *Nup133*$^{-/-}$ (#14)	This paper	N/A

Table S3, related to Experimental Procedures. **Sequences of gRNAs and Primers used in this study:**	SOURCE	IDENTIFIER
gRNA mNup133#1 cgaaaagggaagaaaccctc	This paper	N/A
gRNA mNup133#2 gtcccctactagtgacctca	This paper	N/A
tru gRNA mNup133#5 tacatagtgcacaccagc	This paper	N/A
tru gRNA mNup133#6 tacatagtgcacaccagc	This paper	N/A
mouse Nup133 exon 4 forward primer (Ex4) : GATTTGGTGGCCCTGTCTTA	This paper	N/A
mouse Nup133 reverse primer spanning exons 5/6 (Ex5/6): GAAACTTCCTCCCTGCACTG	This paper	N/A
mouse Nup133 exon 22 forward primer (Ex22): AGTGCAATGCCTGTGTTGAC	This paper	N/A
mouse Nup133 exon 25 reverse primer (Ex25): GCCATCTGAACCAGACCAGT	This paper	N/A
mouse Tbp forward Primer: GAAGAACAATCCAGACTAGCAGCA	(Veazey and Golding, 2011)	N/A
mouse Tbp reverse Primer: CCTTATAGGGAACTTCACATCACAG	(Veazey and Golding, 2011)	N/A

Table S4, related to Experimental Procedures. Antibodies used in this study:	Dilution used *	SOURCE	IDENTIFIER
*IF: immunofluorescence; SR: super resolution; WB: western blot			
Primary antibodies:			
Rabbit monoclonal antibody anti-Nup98.	IF: 1/200 SR: 1/100 WB: 1/1,000	Cell signaling	C39A3 #2598
AlexaFluor 488 NUP98 (C39A3) Rabbit mAb (Alexa Fluor® 488 Conjugate)	SR: 1/150	Cell Signaling Technology	#13358
Rat monoclonal anti-Nup98	WB: 1/2,000	Abcam	ab50610
Rabbit polyclonal antibody anti-Tpr	IF: 1/200 SR: 1/150 WB: 1/500	Abcam	ab84516
Rabbit polyclonal antibody anti-hTpr (VC-2002)	IF: 1/600	From V. Cordes (Kuznetsov et al., 2002)	N/A
Mouse monoclonal antibody anti-Nup153 SA1.	IF: 1/5	from B. Burke (Bodoor et al., 1999)	N/A
	SR: 1/300	Abcam	ab96462
Rat monoclonal anti-mouse Nup133 antibody #74; clone 9C2)	IF: 1/100	Berto et al., submitted	#74; clone 9C2
Rat monoclonal anti-mouse Nup133 antibody #75; clone 3C11G6, was generated against recombinant histidine-tagged mouse Nup133 [aa 66-512] and produced by Proteogenics (Oberhausbergen, France); this antibody does not recognise human Nup133.	WB: 1/10	This paper	#75; clone 3C11G6
Rabbit polyclonal antibody anti-Nup96 (directed against aa 1291-1482 of Nup196)	IF: 1/200	From Beatriz Fontoura (Fontoura et al., 1999)	N/A
Rabbit polyclonal anti-Nup96 antibody	WB: 1/2,000	Bethyl Laboratories	A301-784A
Mouse monoclonal antibody anti-GFP	WB: 1/1,000	Roche Diagnostics	#1.814.460
Mouse monoclonal antibody anti-gamma-tubulin	WB: 1/50,000	Abcam	Ab11316
Mouse monoclonal anti-Cyclin B1 antibody (GNS1)	SR: 1/100	Santa Cruz Biotechnology	sc-245
Rabbit polyclonal anti-hNup107-C serum	WB: 1/2,000	(Belgareh et al., 2001)	#520-82
Rabbit polyclonal anti-mNup85 serum	WB: 1/3,000	From D. Forbes (Harel et al., 2003)	N/A
Rabbit polyclonal anti-GAPDH	WB: 1/2,000	Trevigen	2275-PC100
Secondary antibodies:			
AlexaFluor 488 donkey anti-rabbit	SR: 1/500 IF: 1/1000	ThermoFisher Scientific / Molecular Probes	A21206
AlexaFluor 568 donkey anti-mouse	SR: 1/500	ThermoFisher Scientific	A10037
AlexaFluor 488 donkey anti-mouse	SR: 1/500 IF: 1/1000	ThermoFisher Scientific / Molecular Probes	A21202
AlexaFluor 568 donkey anti-rabbit	SR: 1/500	ThermoFisher Scientific	A10042
AlexaFluor 488 goat anti-mouse	IF: 1/1000	ThermoFisher Scientific	A11029
Cy™3 AffiniPure Donkey Anti-Rabbit	IF: 1/1000	Jackson ImmunoRes.	711-165-152
Cy™3 AffiniPure Donkey Anti-mouse	IF: 1/1000	Jackson ImmunoRes.	715-165-151
Cy™5 AffiniPure Donkey Anti-Rat (all Figs)	IF: 1/1000	Jackson ImmunoRes.	712-175-153
Cy™5 AffiniPure goat anti-mouse	IF: 1/1000	Jackson ImmunoRes.	115-175-068
Cy™3 AffiniPure goat anti-rabbit	IF: 1/1000	Jackson ImmunoRes.	111-165-144
Peroxidase AffiniPure Donkey Anti-Rabbit	WB: 1/5,000	Jackson ImmunoRes.	711-035-152
Peroxidase AffiniPure Goat Anti-mouse	WB: 1/5,000	Jackson ImmunoRes.	115-035-068
Peroxidase AffiniPure Goat Anti-Rat	WB: 1/5,000	Jackson ImmunoRes.	112-035-167

Supplemental Experimental Procedures

Plasmids

Plasmids used in this study are listed in Table S1. They were either previously published or generated using standard molecular cloning techniques including restriction digestions (Fastdigest, Thermo scientific), PCR amplification using proofreading DNA polymerases (Phusion HF, New England Biolab) and In-Fusion HD Cloning Kit (Clontech) or NEBuilder HiFi DNA Assembly Cloning Kits (New England Biolab). The Cas9 vectors (pX-98, pX-102) were assembled by golden gate cloning (Engler et al., 2009). For all constructs, PCR-amplified fragments and junctions were checked by sequencing. Plasmid maps are available upon request.

mESC lines derivation, growth conditions, and transfection

Cell lines used in this study are listed in Table S2. All cells were grown at 37°C and 5% CO_2.

DR4-mouse embryonic fibroblast feeder cells, DR4-MEFs (Applied StemCells), were grown in Dulbecco's Modified Eagle's Medium (DMEM) (Gibco) supplemented with 15% heat-inactivated fetal bovine serum (FBS, Gibco), 100U/ml Penicillin-100μg/ml Streptomycin (P/S) (Gibco) and 2mM L-Glutamine (Gibco). DR4-MEFs were inactivated using 8.5μg/ml Mitomycin-C (Sigma-Aldrich) for 3 hours.

mESCs were grown in serum/leukemia inhibitory factor (LIF)-containing stem cell medium: DMEM + L-glutamine + 15% heat-inactivated ESC-Qualified FBS (Gibco), 2-mercaptoethanol (Gibco) and 10^3 units/ml LIF (ESGRO, Millipore). The medium used for early passages cell lines (1A4, JA1, #319 and #532) also contained non-essential amino acids.

HM1 (Selfridge et al., 1992) and derivative mESCs clones were grown in the serum/LIF-containing medium supplemented with non-essential amino acids (Gibco), and nucleosides (Millipore). Except for 3D-SIM imaging, mESCs were grown on inactivated DR4-MEFs (MEF-derived feeders) plated on 0.1% gelatin (Sigma-Aldrich) and were passaged every 2 or 3 days using 0.05% Trypsin (Gibco).

For SIM imaging, early passage (3-to-6) mESCs were thawed onto a plate of MEF derived feeders in serum/LIF-containing stem cell medium (as above) and allowed to grow for two to three days before replacing the medium with a 1:1 mixture of serum/LIF and 2i/LIF stem cell media: 50% DMEM/F12; 50% Neurobasal Medium; plus L-glutamine, P/S, BSA, and 2-mercaptoethanol at concentrations recommended by ThermoFisher Scientific; N2

(ThermoFisher 0.5X); B27 (ThermoFisher 0.5X); 3 μM CHIR99021 (Stemgent); 1 μM PD0325901 (Stemgent); and ESGRO mLIF 10^3 units/ml. Cells were subsequently maintained without feeders in 2i plus LIF medium on fibronectin-coated plates (2.5 μg/ml in PBS, incubated overnight at 37°C) up to passage #10.

For transfections, 5.10^5 mESCs were plated onto DR4-MEFs in 35mm dishes in medium without P/S. Plasmid DNA (3μg) and Lipofectamine 2000 (Invitrogen) were mixed in OptiMEM (Invitrogen) and added to the cells according to the manufacturer's instructions. Transiently transfected cells were analyzed for iFRAP, immunostaining or western blot 48h post transfection.

To establish *Nup133*$^{-/-}$ mESCs stably expressing GFP- or mCherry-tagged Nup133-FL, -ΔN, -ΔC or -ΔMid, 1μg/ml of puromicin (Invivogen) was added to culture medium 24h after transfection, individual puromicin-resistant colonies were then individually picked after 7 to 10 days, dissociated with tryspin and plated on 96-well plates containing DR4-MEFs. Clones selected on the basis of fluorescence level and NE localization of the GFP/mCherry fusion and Nup133 immunostaining, were further characterized for the proper size and expression level of the fusion protein by western blot. Selected clones were continuously grown in the presence of 0.5 μg/ml puromycin.

Nup133$^{-/-}$ (#14) mESCs were derived from HM1 cells by CRISPR/Cas9 editing. Briefly, HM1 mESCs were co-transfected with two plasmids directing the expression of two gRNAs or two tru-gRNAs (Fu et al., 2014) targeting Nup133 either around exon 2 or within exon 6, along with Cas9 (wt or nickase version) fused to EGFP or mCherry. Tru-gRNAs were designed using the MIT website (http://www.genome-engineering.org/) and are listed in Table S3. Two days after transfection, cells were sorted by Fluorescence-activated cell sorting (FACS) based on GFP and mCherry expression, grown for 4 days, and plated at low concentration on inactivated DR4-MEFs-coated plates. Individual clones were picked after 6 days and were first selected based on the lack of Nup133 expression by immunostaining using anti NTD and anti-CTD Nup133 antibodies (16 out of 19 clones were Nup133-negative). Selected clones were subsequently characterized by PCR on genomic DNA followed by sequencing.

Real-time quantitative PCR

Total RNAs were extracted from mESCs by using the NucleoSpin RNAII isolation kit (Machery-Nagel), and mRNAs were reverse transcribed and amplified using random hexamers (Amersham Pharmacia) and the SuperScript II reverse transcriptase kit (Invitrogen). Real-time quantitative PCR was performed on the resulting cDNAs with a LightCycler480 instrument (Roche Life Sciences) by using SYBR Green incorporation (SYBR Green PCR-Master Mix; Applied Biosystems) and specific primer pairs (listed in Table S3). The relative amounts of cDNAs in the samples were quantified according to the manufacturer's instructions and normalized by reference to the TATA-binding protein (*Tbp*) cDNAs.

Detailed procedures from High Resolution Imaging (3D SIM): immunostaining, image acquisition and processing

For 3D SIM imaging, mESCs were washed in PBS(+) ($Ca^{2+}Mg^{2+}$) and then fixed in 4% paraformaldehyde for 15 minutes at room temperature (RT). After 3 subsequent washes in PBS(-) (no $Ca^{2+}Mg^{2+}$), cells were permeabilized in IF-Perm Buffer [PBS(-) plus 0.2% Triton X-100] for 6 min at RT. Following three more washes in PBS(-), cells were incubated in IF Wash Buffer [PBS(-) plus 3% IgG-free BSA and 0.1% Triton X-100] for 30 to 60 min. Incubation with primary antibody was carried out in IF Wash Buffer for ~3 hours at RT or at 4ºC overnight. Cells underwent 4-to-5, five-minute washes in IF Wash Buffer before incubation with Alexafluor-conjugated donkey or goat antibodies (ThermoFisher, 1:500 dilution) plus 5ng/ml DAPI (ThermoFisher) for 45 minutes to 1 hour at RT. Depending on the species of the secondary antibody, the IF Wash Buffer for this incubation included 3% donkey or goat serum. Subsequently cells underwent 3-to-4, five-min washes in IF Wash Buffer and then 2, five-min washes in PBS(-) before mounting on slides with Prolong Gold (ThermoFisher). For incubation with 2 rabbit antibodies (anti-Tpr, anti-Nup98; as in Fig 2C), incubations were done sequentially as follows: Initial antibody incubation and washes were with rabbit anti-Tpr as above, followed by Alexafluor 568-conjugated donkey anti-rabbit IgG plus DAPI. After the PBS washes, there was an additional ~1 hr. incubation with IF wash buffer containing 3% normal rabbit serum, to block any remaining donkey anti-rabbit secondary antibody. Finally, rabbit anti-Nup98, preconjugated to AlexaFluor 488; (Cell Signaling Technology) was incubated, followed by final washes and mounting.

Prior to performing single pore quantitation, the specificity of the antibodies to Tpr, Nup98 and Nup153 was assessed by co-staining with antibodies to Lamin B1, a marker of the nuclear envelope (NE). Antibodies selected for pore quantitation produced negligible intra and extra-nuclear staining; enabling visual definition of the nuclear boundary without a Lamin B1 marker. Control staining in the absence of primary antibody was performed to confirm that the secondary antibody also generated minimal background.

3D-SIM super-resolution microscopy was performed using a DeltaVision OMX V4/Blaze 3D-SIM super-resolution microscope (GE Healthcare) housed in the Rockefeller University's Bio-Imaging Resource Center (BIRC). This OMX system was fitted with a 100x/1.40 UPLSAPO oil objective (Olympus); Evolve EMCCD cameras (Photometrics) were used in EM gain mode at a gain of 170, with 405nm, 488 nm and 568 nm laser lines for excitation, and 436/31, 528/48 and 609/37 nm emission filters, respectively. Optical sections were acquired at 125-nm intervals. Immersion oil refractive index (R.I.) was selected to optimize for the 568 nm channel and the ambient temperature. Structured illumination data sets were reconstructed using softWoRx software (GE Healthcare), employing optical transfer functions (OTFs) generated from point spread functions acquired from 100 nm FluoSpheres (green or red) or 170 nm PS-Speck beads (blue) (ThermoFisher) using oil with the R.I. optimized for the 568 nm channel, according to procedures described in (Demmerle et al., 2017). Reconstruction of the structured illumination data sets used channel-specific k0 values, custom OTFs, and Wiener filters of 0.005, 0.002, and 0.002 for the blue, green, and red channels, respectively. Image registration was performed with parameters that had been refined using 100-nm TetraSpeck beads (ThermoFisher). Image registration parameters and OTFs were frequently refined by the BIRC staff, and checked using antibodies to TPR stained with both red (568) and green (488) secondary antibodies in parallel. The effective pixel size of the reconstructed images is 40nm in xy.

Western blot analyses

To prepare whole cell lysates, mESCs were lysed in 2× Laemmli lysis buffer (150-mM Tris-HCL (pH 6.8), 5 % (wt/vol) SDS, 25 % (vol/vol) glycerol, and 0.01 % (wt/vol) bromophenol blue). Lysates were incubated for 3 min at 95 °C, clarified by sonication (Bioruptordiagenode: 3 cycles of 30 s on/off, high power), and denatured again for 3 min at 95°C. Protein concentration was then determined using a BCA assay kit (Thermo Scientific).

Total protein extracts supplemented with β-mercaptoethanol (750 mM final, Sigma-Aldrich) were analyzed by western blot.

10 μg of mESC lysate were separated on 4–12% or 10% SDS-PAGE gels (pre-cast NuPage® GE healthcare) and transferred to nitrocellulose (GE healthcare) or PVDF (Millipore) membranes. The resulting blots were stained using Ponceau, saturated with TBS, 0.1% Tween, and 5% dried milk, and probed with antibodies of interest (listed in Table S4)**.** Incubations of the membrane with primary and HRP-conjugated secondary antibodies (Jackson ImmunoResearch Laboratories) were done in TBS buffer (0.1 % Tween, 5 % dried milk), and signals were detected by enhanced chemiluminescence (SuperSignal® Pico or Femto, ThermoScientific) using Las-4000 mini (Fujifilm).

Pull-down experiments and mass spectrometry analyses:

Rosetta bacteria transformed with the pET28a-zz-hNup153 vectors (aa 1-245 or 1-339) generously provided by D. Forbes (Vasu et al., 2001), were used to produce the His_6-ProtA-Nup153-NTD-His_6 recombinant proteins. After transformation, bacteria were grown at 37°C in 1 liter of LB +25μg/ml Chloramphenicol + 50μg/ml Kanamycin up to 0.3 OD_{600}/ml and transferred for 1h at 23°C. Expression of the recombinant proteins was then induced by addition of 0.5 M IPTG and growth at 23°C over-night. The following day, bacteria were pelleted and lysed in cold PBS + 0.2 % Triton X100 + 1 mM DTT + Pi solution (protease inhibitors; 100x stock solution: 0.4 mg/mL pepstatin A and 18mg/mL PMSF in ethanol)+ 10 mM Imidazole (5 mL per 150 OD_{600}) using a rapid freeze-and-thaw cycle followed by sonication. Bacterial lysates were centrifuged at 4°C, 12000 g for 10 min and the supernatant was incubated with pre-washed and equilibrated nickel beads (30 μl – QIAGEN GmbH Ni-NTA Agarose Beads per mL of bacterial lysate) for 1 hour at 4°C. Nickel beads were then washed 3 times with high salt mESC lysis buffer (400mM NaCl, 20mM TRIS pH 7.5, 1mM DTT, 1.2% TritonX100, 0.5% Tween20, 1mM MgCl2, Pi solution) + 20mM imidazole, once with PBS and saturated by a 30-min incubation in PBS + 1% BSA, followed by two washes in Washing buffer (100mM NaCl, 20mM TRIS pH 7,5 + 1mM DTT + 0.3% triton Tx100 + 0.5% Tween20, 1mM MgCl2) + 20mM imidazole.

In the meantime, mESC lysates were prepared by resuspending a frozen pellet of $4x10^6$ mESCs (~500μg total proteins) in 200 μl of high salt mESC lysis buffer + 10mM imidazole. Following 10 min incubation at 4°C, lysates were centrifuged at 16.000 g for 30 min at 4°C. The resulting supernatant was diluted four times in a low-salt buffer (20 mM TRIS pH 7.5, 1

mM DTT, 10mM imidazole, 0.5% Tween20, Pi solution) and pre-cleared by a 30-min incubation with nickel beads equilibrated with washing buffer + 10mM imidazole. The resulting cleared supernatant (input) was then incubated for 2 hours at 4°C with 30μL of the His_6-ProtA-Nup153-NTD-His_6-coated nickel beads. After incubation, beads were extensively washed with Washing buffer +20 mM imidazol. The proteins were then eluted in 50μL of Laemmli and boiled 3 minutes for subsequent western blot analyses. Alternatively, the beads were washed with 20 mM $(NH_4)_2CO_3$ and 10 μL were processed for mass-spectrometry analysis.

LC-MS/MS acquisition and analysis**:** Proteins on beads were incubated overnight at 37°C with 20 µL of 25 mM NH_4HCO_3 containing sequencing-grade trypsin (12.5 µg/mL; Promega). The resulting peptides were desalted using ZipTip μ-C18 Pipette Tips (Millipore) and analyzed in technical triplicates by a Q-Exactive Plus coupled to a Nano-LC Proxeon 1000 equipped with an easy spray ion source (all from Thermo Scientific). Peptides were separated by chromatography with the following parameters: Acclaim PepMap100 C18 pre-column (2 cm, 75 µm i.d., 3 µm, 100 Å), Pepmap-RSLC Proxeon C18 column (50 cm, 75 µm i.d., 2 µm, 100 Å), 300 nl/min flow rate, gradient from 95 % solvent A (water, 0.1 % formic acid) to 35 % solvent B (100 % acetonitrile, 0.1% formic acid) over a period of 98 minutes, followed by a column regeneration for 23 min, giving a total run time of 2 hours. Peptides were analyzed in the Orbitrap cell, in full ion scan mode, at a resolution of 70,000 (at *m/z* 200), with a mass range of *m/z* 375-1500 and an AGC target of 3 $x10^6$. Fragments were obtained by high collision-induced dissociation (HCD) activation with a collisional energy of 30%, and a quadrupole isolation window of 1.4 Da. MS/MS data were acquired in the Orbitrap cell in a Top20 mode, at a resolution of 17,500, with an AGC target of $2x10^5$, with a dynamic exclusion of 30 seconds. MS/MS of most intense precursor were firstly acquired. Peptides with unassigned charge states or monocharged were excluded from the MS/MS acquisition. The maximum ion accumulation times were set to 50 ms for MS acquisition and 45 ms for MS/MS acquisition.

Raw LC-MS/MS data from the Q-Exactive Plus were analyzed using the MaxQuant software (Cox and Mann, 2008) version 1.6.0.1, which includes the Andromeda search engine (Cox et al., 2011). Spectra were matched to peptides from the mouse proteome database downloaded from Uniprot. Quantifications were performed using MaxLFQ (Cox et al., 2014) on proteins identified with at least two peptides with a False Discovery Rate (FDR) < 0.05. LFQ values were further analyzed using the Perseus software (version 1.6.0.2). For the

statistical analyses of immunoprecipitations, three replicates of each condition were separated into statistical groups and a Student's *t* test was performed. Results are presented as Volcano-plots (Hubner and Mann, 2011) with a threshold set with an FDR < 0.05 and an S_0 of 2.

References to Supplemental Experimental Procedures:

Belgareh, N., Rabut, G., Bai, S.W., van Overbeek, M., Beaudouin, J., Daigle, N., Zatsepina, O.V., Pasteau, F., Labas, V., Fromont-Racine, M., *et al*. (2001). An evolutionarily conserved NPC subcomplex, which redistributes in part to kinetochores in mammalian cells. J Cell Biol *154*, 1147-1160.

Bodoor, K., Shaikh, S., Salina, D., Raharjo, W.H., Bastos, R., Lohka, M., and Burke, B. (1999). Sequential recruitment of NPC proteins to the nuclear periphery at the end of mitosis. J Cell Sci *112 (Pt 13)*, 2253-2264.

Cox, J., Hein, M.Y., Luber, C.A., Paron, I., Nagaraj, N., and Mann, M. (2014). Accurate proteome-wide label-free quantification by delayed normalization and maximal peptide ratio extraction, termed MaxLFQ. Mol Cell Proteomics *13*, 2513-2526.

Cox, J., and Mann, M. (2008). MaxQuant enables high peptide identification rates, individualized p.p.b.-range mass accuracies and proteome-wide protein quantification. Nat Biotechnol *26*, 1367-1372.

Cox, J., Neuhauser, N., Michalski, A., Scheltema, R.A., Olsen, J.V., and Mann, M. (2011). Andromeda: a peptide search engine integrated into the MaxQuant environment. J Proteome Res *10*, 1794-1805.

Demmerle, J., Innocent, C., North, A.J., Ball, G., Muller, M., Miron, E., Matsuda, A., Dobbie, I.M., Markaki, Y., and Schermelleh, L. (2017). Strategic and practical guidelines for successful structured illumination microscopy. Nat Protoc *12*, 988-1010.

Engler, C., Gruetzner, R., Kandzia, R., and Marillonnet, S. (2009). Golden gate shuffling: a one-pot DNA shuffling method based on type IIs restriction enzymes. PLoS One *4*, e5553.

Fontoura, B.M., Blobel, G., and Matunis, M.J. (1999). A conserved biogenesis pathway for nucleoporins: proteolytic processing of a 186-kilodalton precursor generates Nup98 and the novel nucleoporin, Nup96. J Cell Biol *144*, 1097-1112.

Fu, Y., Reyon, D., and Joung, J.K. (2014). Targeted genome editing in human cells using CRISPR/Cas nucleases and truncated guide RNAs. Methods Enzymol *546*, 21-45.

Harel, A., Orjalo, A.V., Vincent, T., Lachish-Zalait, A., Vasu, S., Shah, S., Zimmerman, E., Elbaum, M., and Forbes, D.J. (2003). Removal of a single pore subcomplex results in vertebrate nuclei devoid of nuclear pores. Mol Cell *11*, 853-864.

Hubner, N.C., and Mann, M. (2011). Extracting gene function from protein-protein interactions using Quantitative BAC InteraCtomics (QUBIC). Methods *53*, 453-459.

Kuznetsov, N.V., Sandblad, L., Hase, M.E., Hunziker, A., Hergt, M., and Cordes, V.C. (2002). The evolutionarily conserved single-copy gene for murine Tpr encodes one prevalent isoform in somatic cells and lacks paralogs in higher eukaryotes. Chromosoma *111*, 236-255.

Rabut, G., Doye, V., and Ellenberg, J. (2004). Mapping the dynamic organization of the nuclear pore complex inside single living cells. Nat Cell Biol *6*, 1114-1121.

Selfridge, J., Pow, A.M., McWhir, J., Magin, T.M., and Melton, D.W. (1992). Gene targeting using a mouse HPRT minigene/HPRT-deficient embryonic stem cell system: inactivation of the mouse ERCC-1 gene. Somat Cell Mol Genet *18*, 325-336.

Vasu, S., Shah, S., Orjalo, A., Park, M., Fischer, W.H., and Forbes, D.J. (2001). Novel vertebrate nucleoporins Nup133 and Nup160 play a role in mRNA export. J Cell Biol *155*, 339-354.

Veazey, K.J., and Golding, M.C. (2011). Selection of stable reference genes for quantitative rt-PCR comparisons of mouse embryonic and extra-embryonic stem cells. PLoS One *6*, e27592.

Whittle, J.R., and Schwartz, T.U. (2009). Architectural nucleoporins Nup157/170 and Nup133 are structurally related and descend from a second ancestral element. J Biol Chem *284*, 28442-28452.